

S- and C-band nanosecond 1×2 plasma dispersion $3\text{-}\mu\text{m}$ silicon MZI switch with low polarization sensitivity

Yu Wang

ECO Group, Eindhoven Hendrik
Casimir Institute
Eindhoven University of Technology
Eindhoven, The Netherlands
y.wang13@tue.nl

Srivathsa Bhat

VTT Technical Research Centre of
Finland Ltd.
Espoo, Finland
srivathsa.bhat@vtt.fi

Timo Aalto

VTT Technical Research Centre of
Finland Ltd.
Espoo, Finland
timo.aalto@vtt.fi

Nicola Calabretta

ECO Group, Eindhoven Hendrik
Casimir Institute
Eindhoven University of Technology
Eindhoven, The Netherlands
n.calabretta@tue.nl

Abstract— We fabricated and assessed a nanosecond 1×2 electro-optic MZI switch on $3\text{-}\mu\text{m}$ thick silicon platform. The device has 0.9dB insertion loss, 19dB average extinction ration, <0.7dB polarization dependent loss and 6-ns switching time.

Keywords— optical switch, silicon photonics, integrated optics

I. INTRODUCTION

Wideband transmission can increase the capacity beyond C- band up to tenfold by exploiting the low-loss region from O- to L- band of a single mode fiber (ITU-T G.652.D) [1]. To efficiently manage the large heterogeneous data traffic in wideband optical network, wideband photonic integrated wavelength selective switch (WSS) is the promising solution to implement a programmable network by flexibly routing wavelengths from different inputs to desired outputs without electric-optic conversion [2]. For managing the dynamic data traffic in all-optical wideband network, the WSS needs to have low wavelength/polarization sensitivity, fast switching operation, high extinction ratio and low insertion loss. Current commercial WSSs employ free-space optics and micro-electro-mechanical system technology, but it is difficult for mass producing due to complex assembly and they have bulky footprint and high cost. The WSS based on photonic integrated technology is the other attractive option, because it has compact size, low price, high stability and mass productivity. The typical photonic integrated WSS consists of on-chip demultiplexer/multiplexer for wavelength separation/combining and the switching unit for passing/blocking the channels. Many switching units with different types are designed and fabricated on different integrated photonic platforms: 1×2 Mach Zehnder Interferometer (MZI) switch for 1×2 WSS design using thermo-optic effect is realized on silica platform in [3], but it has disadvantages of high polarization sensitivity, slow switching speed and large chip footprint; 1×2 thermo-optic polymer switch based on total internal reflection effect has low wavelength/polarization sensitivity, but several milliseconds switching time [4]. 220-nm thick silicon electro-optic MZI switch has compact size and nanosecond switching speed, but it works only for single polarization (TE mode) [5]. 1×2 MZI switch with electro-optic phase shifter on $3\text{-}\mu\text{m}$ silicon platform can provide wideband polarization insensitive (PI) and nanosecond

switching operation benefiting from the $3\text{-}\mu\text{m}$ thick silicon waveguide's down-to-zero birefringence [6]. Moreover, the

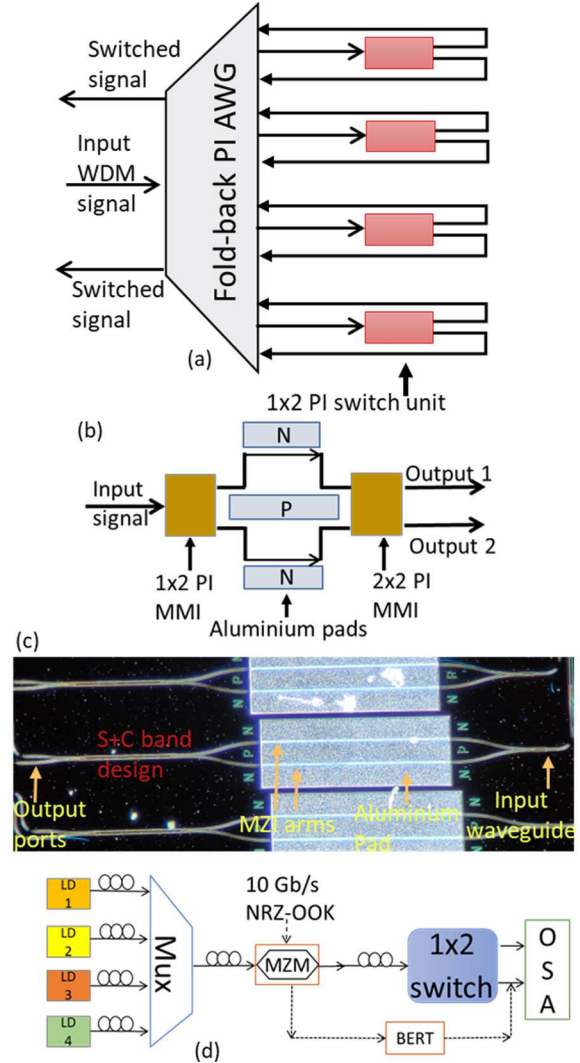


Fig. 1. (a) the configuration of 1×2 wideband PI WSS; (b) the structure of the 1×2 PI switch; (c) the micrograph of the fabricated chip; (d) the experiment set-up.

1×2 PI switch unit can be co-integrated with PI AWGs as demultiplexer/multiplexer [7] to realize a photonic integrated PI WSS on 3- μm silicon platform (the configuration is shown in Fig. 1 (a)).

In this work, we demonstrate a fabricated wideband (S- to C-band) 1×2 electro-optic MZI switch on 3- μm silicon platform with nanosecond switching speed, low polarization sensitivity, low insertion loss and high extinction ratio. The experimental results show that in the S- and C-band the 1×2 switch has insertion losses ranging from 1.8 dB to 2.7 dB (for TE) and 1.1 dB to 1.9 dB (for TM), polarization dependent loss (PDL) < 0.7 dB, 19 dB average extinction ratio between output 1/2, 6 ns switching rising time and 8 ns falling time. The device requires only 0.35V RF switching voltage that results in 65 mW power consumption. Transmission experiments have been performed and results show error free operation with < 0.2 dB power penalty at 10^{-9} BER for 10 Gbit/s data.

II. DESIGN OF THE 1×2 SWITCH

The structure of the 1×2 PI electro-optic MZI switch is illustrated in Fig. 1 (b), it consists of a 1×2 multi-mode interferometer (MMI) as the input power splitter, two phase shifters (MZI arms) and a 2×2 MMI as the output power coupler. The photonic integrated chip is designed and fabricated on the 3- μm thick silicon platform with ultra-low optical loss (~ 0.1 dB/cm) and dense integration of μm -scale

bends [6]. The 1×2 MMI is designed to have 50:50 power splitting ratio and PI operation, and its output ports connects equal-length phase shifters. The 1-mm long PIN MZI arm provides PI phase changing benefitting from the zero birefringence of $3\ \mu\text{m} \times 3\ \mu\text{m}$ strip waveguide. The rib-strip converter is placed between the multi-mode strip waveguide and the single-mode rib waveguide to avoid high-mode excitation in the strip waveguide, and the light beam is coupled from the fiber to the rib waveguide. The $100\ \mu\text{m} \times 1000\ \mu\text{m}$ aluminum pads are placed on the side of the phase shifters for introducing driving voltage. The PI 2×2 MMI connects the phase shifters and works as the 3-dB coupler. The controlling of carrier concentration is based on plasma dispersion effect and realized by carrier injection with the forward biased PIN junction. When the phase-shift waveguide is operated with forward bias voltage through aluminium pad (only one arm is driven during switching), carriers are injected into the waveguide and the refractive index changes. By changing driving voltage and adjusting the phase difference between two MZI arms, the input optical signal can be switched to one of the two output ports with nanoseconds speed (benefitting from the highly efficient electro-optic effect of the silicon platform). The microscope image of the fabricated chip is shown in Fig. 1 (c).

III. EXPERIMENTAL RESULTS

Fig. 1 (d) shows the experimental set-up for assessing the 1×2 PI electro-optic switch with S- and C-band optical signals.

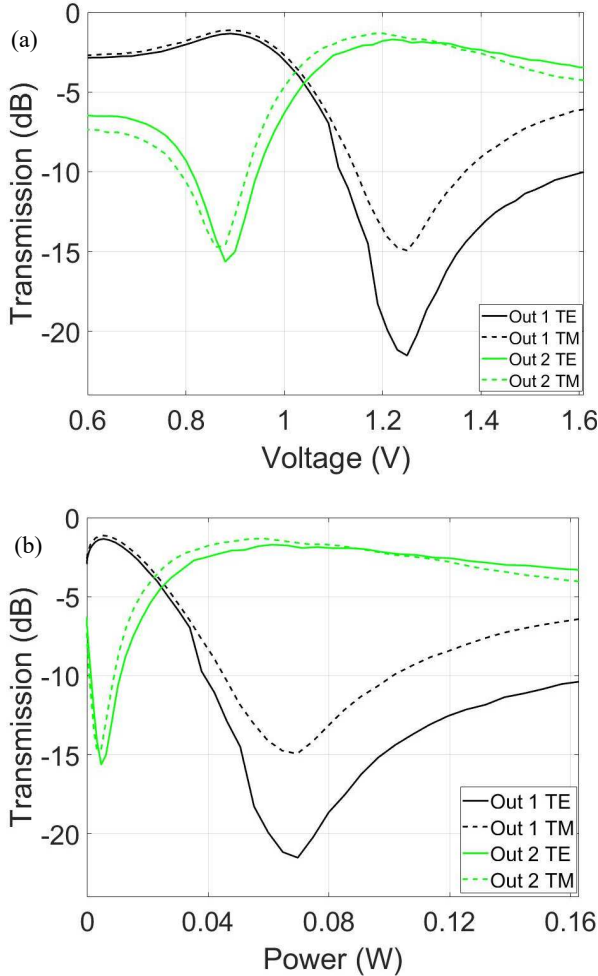


Fig. 2. (a) transmission versus voltage curves; (b) transmission versus power curves.

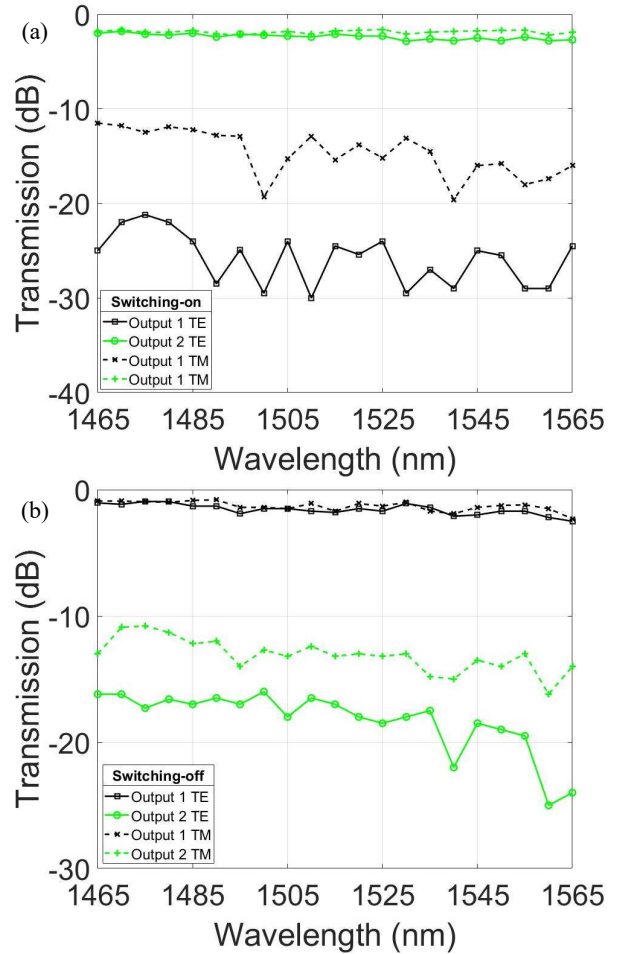


Fig. 3. Output spectrum from 1465 nm to 1565 nm for switching on (a) and off (b).

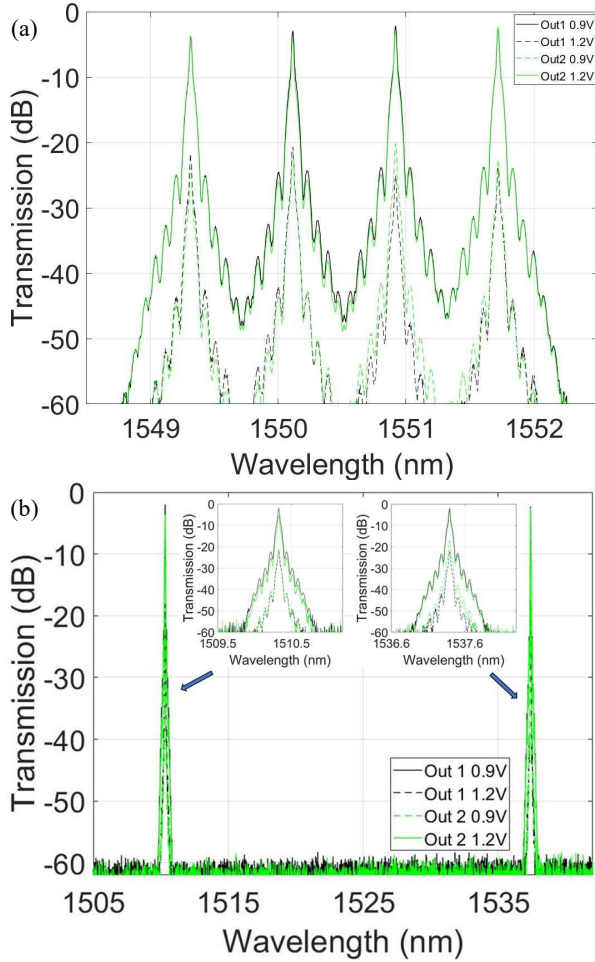


Fig. 4. Switched spectra of 10 Gb/s WDM signal at (a) 100 GHz spacing and (b) 3.5 THz spacing.

Firstly, the switching on/off spectra of two output ports for the TE/TM polarizations were measured. A wideband tunable laser source and a polarization controller were used to measure the polarization dependent performance. DC driving voltage was provided through the aluminium pads via probes to the chip, and the DC forward-bias voltage was applied on one arm of the switch. Fig. 2 (a) shows the measured switching transmission characteristics for 1496 nm as a function of applied bias voltage with TE/TM modes. In the switching-off state, a low insertion loss at output 1 of 1.1 dB for TE (1.3 dB for TM) with a PDL < 0.2 dB and the extinction ratio between output 1 and 2 of 14.5 dB for TE (13.6 dB for TM) were measured. For the switching-on state, the insertion loss of output 2 was around 1.8 dB for TE (1.3 dB for TM), the PDL was < 0.5 dB, and the extinction ratio was around 20.1 dB for TE (13.4 dB for TM). The switching-on requires 0.35 V (with 0.88 V DC bias) which results in a power consumption of about 65 mW. To verify the wideband operation of the device, the switching on/off performance were recorded from 1465 nm to 1565 nm for TE/TM modes. Fig. 3 (a) and (b) show that the insertion losses of output 1 range from 1.7 dB to 2.8 dB for TE at the switching-on state (from 1.6 dB to 2.2 dB for TM), and range from 1.0 dB to 2.5 dB for TE (from 0.9 dB to 2.3 dB for TM) at output 2 at switching-on state. The PDLs are from 0.1 dB to 0.7 dB. The extinction ratios of output 1 and output 2 for switching on and off range from 19.3 dB to 28.0 dB for TE (from 10.2 dB to 17.3 dB for TM), from 14.8 dB to 23.5 dB at TE (10.0 dB to 14.9 dB at TM), respectively.

Furthermore, the switching performance has been assessed for 10 Gbit/s NRZ-OOK 100 GHz spaced WDM channels (ITU grid 35 to 32: 1549.32 nm, 1550.12 nm, 1550.92 nm and 1551.72 nm) and 3.5 THz spacing WDM signal (1510.29 nm and 1537.4 nm). The spectra of switched modulated WDM signal from output 1 and output 2 are illustrated in Fig. 4 (a) and (b) for 100 GHz spacing and 3.5 THz spacing, respectively. The black curves and green curves represent output spectrum from output 1 and output 2, respectively, with solid curves for 0.9 V driving voltage and dashed curves for 1.2 V voltage. Fig. 4 (a) shows the 100 GHz WDM signal's average extinction ratio of 17 dB for switching-off state and 22 dB for switching-on state with 10 Gbit/s data rate. The 3.5 THz WDM signal has 16.2 dB averaged extinction ratio for switching-off and 19.5 dB averaged extinction ratio for switching-on (see Fig. 4 (b)). The switching rising and falling time is also recorded by the oscilloscope and shown in Fig. 5 (a) with around 6 ns rising time and around 8 ns falling time.

To quantify the chip's performance with data transmission, BER of modulated signals at high data rates were measured

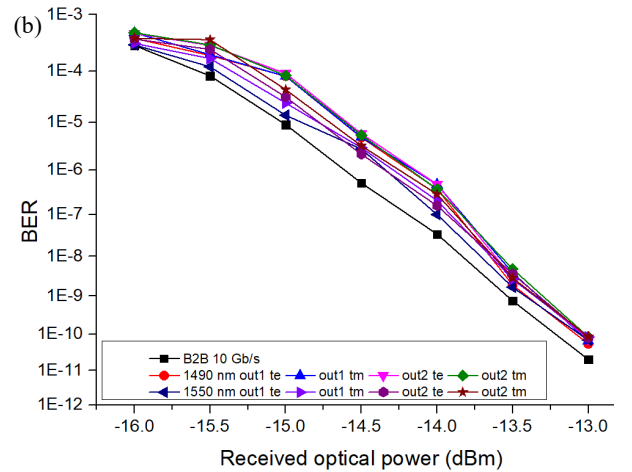
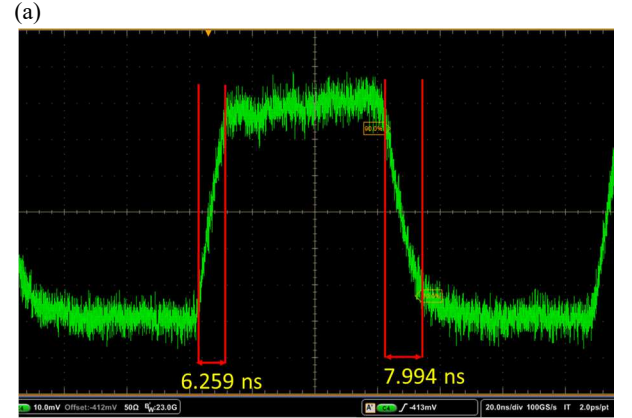


Fig. 5. (a) the switching rising/falling time; (b) BER curves at 10 Gb/s.

with 10 Gbit/s NRZ-OOK signal (PRBS $2^{31}-1$). The back-to-back (B2B) BER curve is reported as reference. Results show error free operation with < 0.2 dB power penalty at 10^{-9} BER for switched on/off 10 Gbit/s signal at 1490 nm and 1550 nm to output 1 and 2 (see Fig. 5 (b)).

IV. CONCLUSION

We experimentally demonstrated a polarization insensitive S- to C- band 1×2 electro-optic switch. The experimental results show that from 1465 nm to 1565 nm the device has the lowest insertion losses of 1.0 dB for TE and 0.9

dB for TM, down to 0.1 dB PDL, the average extinction ratios of ~ 18.7 dB for switching on and 15.8 dB for switching off, 6 ns switching rising time and 8 ns falling time, 0.35 V bias voltage and 65 mW power consumption for switching on. The power penalty of error free operation at 10^{-9} BER is around 0.2 dB for 10 Gb/s data.

ACKNOWLEDGMENT

This work has been partially supported by the EU Horizon 2020 research and innovation programme under the Marie Skłodowska-Curie grant agreement 814276 and the EU B5G-OPEN grant agreement 101016663. And the work is part of the Academy of Finland Flagship Programme, Photonics Research and Innovation (PREIN), decisions 320168 and 346545.

REFERENCES

- [1] A. Ferrari et al., "Assessment on the achievable throughput of multi-band ITU-T G. 652. D fiber transmission systems", *J. Lightw. Technol.*, vol. 38, no. 16, pp. 4279-4291, Aug. 2020.
- [2] N. Calabretta, N. Tessema, K. Prifti, A. Rasoulzadehzali, Yu Wang, S. Bhat, G. Delrosso, T. Aalto, R. Stabile, "Programmable modular photonic integrated switches for beyond 5G metro optical networks," *Proc. SPIE 11690, Smart Photonic and Optoelectronic Integrated Circuits XXIII*, 116900O (5 March 2021); <https://doi.org/10.1117/12.2580374>
- [3] R. M. G. Kraemer et al., "High Extinction Ratio and Low Crosstalk C and L-Band Photonic Integrated Wavelength Selective Switching", 2020 22nd International Conference on Transparent Optical Networks (ICTON), pp. 1-4, 2020.
- [4] Y. Wang, J. Shin, N. Tessema, M. Hout, S. Heide, C. Okonkwo, H. Jung, and N. Calabretta, "Ultra-wide band (O to L) photonic integrated polymer cross-bar switch matrix," *Opt. Lett.* 46, 5324-5327 (2021)
- [5] J. Campenhout, et al., "Low-power, 2x2 silicon electro-optic switch with 110-nm bandwidth for broadband reconfigurable optical networks," *Opt. Express* 17, 24020-24029 (2009)
- [6] Y. Wang et al., "Ultrawide-band Low Polarization Sensitivity 3- μ m SOI Arrayed Waveguide Gratings," in *Journal of Lightwave Technology*, vol. 40, no. 11, pp. 3432-3441, 1 June1, 2022, doi: 10.1109/JLT.2022.3167829.
- [7] T. Aalto, et al., "Open-Access 3- μ m SOI Waveguide Platform for Dense Photonic Integrated Circuits," in *IEEE Journal of Selected Topics in Quantum Electronics*, vol. 25, no. 5, pp. 1-9, Sept.-Oct. 2019, Art no. 8201109. DOI: 10.1109/JSTQE.2019.2908551.